# Structure and Reactivity Studies on Dinuclear Copper Complexes of the Ligand α,α′-Bis{bis[1-(1′-methyl-2′-benzimidazolyl)methyl]amino}-*m*-xylene

**Giuseppe Battaini,[a] Luigi Casella,*[a] Michele Gullotti,[b] Enrico Monzani,[a] Giorgio Nardin,[c] Angelo Perotti,[a] Lucio Randaccio,[c] Laura Santagostini,[b] Frank W. Heinemann,[d] and Siegfried Schindler[d]**

**Keywords:** Bioinorganic chemistry / Copper / Dioxygen activation / Enzyme models

The ligand α,α′-bis{bis[1-(1′-methyl-2′-benzimidazolyl)-methyl]amino}-*m*-xylene (L-55) forms the complexes $[Cu^{I}_2$(L-55)$(MeCN)_2](PF_6)_2$ (**1**) and $[Cu^{II}_2$(L-55)$(OMe)_2][ClO_4]_2$ (**2**), in which an extremely weak axial amine interaction is imposed by the small five-membered benzimidazole chelating ring units. This structural feature has been characterized by X-ray crystal structure determination. In **1**, the $Cu^{I}$ centers are three-coordinate with ligation from two benzimidazolyl and one acetonitrile N-donors, in a slightly distorted trigonal arrangement. In **2**, each $Cu^{II}$ center has a distorted square-planar geometry and coordinates to the benzimidazolyl N atoms and the bridging methoxy groups in the basal positions, with a much weaker interaction with the tertiary amine N in an apical position. These structural features affect the reactivities of the copper(I)– and copper(II)–L-55 complexes toward dioxygen and hydrogen peroxide, respectively. $[Cu^{I}_2$(L-55)$(MeCN)_2]^{2+}$ does not produce a stable peroxo complex, but undergoes an irreversible oxidation to copper(II) species, while $[Cu^{II}_2$(L-55)$(H_2O)_2]^{4+}$ reacts slowly with hydrogen peroxide to undergo regiospecific hydroxylation of the ligand at one benzylic carbon atom, which causes decomposition of the complex. $[Cu_2$(L-55)$(H_2O)_2]^{4+}$ is easily converted into its bis(μ-hydroxo) adduct $[Cu_2$(L-55)$(OH)_2]^{2+}$. This pH-driven equilibrium was monitored by paramagnetic $^1H$ NMR spectroscopy, and the solution magnetic properties of the complexes were determined by the Evans susceptibility method.



## Introduction

The interactions between synthetic copper complexes and dioxygen have become increasingly important in the last decade,[1−4] in connection with the enzymatic reactions catalyzed by copper enzymes,[5−9] particularly tyrosinase, and potential applications in catalytic transformations of organic substrates.[10,11] In the best characterized systems, the μ-$\eta^2$:$\eta^2$-peroxodicopper(II) or bis(μ-oxo)dicopper(III) complexes have been found to be able to effect C−H bond cleavage of the ligand[12−18] or an exogenous substrate[19,20] with insertion of an oxygen atom. In other dinuclear copper systems the putative copper−dioxygen intermediate could not be characterized, due to high reactivity even at low temperature.[21−26] The first and most intensely studied example of a tyrosinase model, $[Cu_2$(*m*-XYLpy$_2$)$]^{2+}$,[12,13,27−29] performs ligand arene hydroxylation, to produce a μ-hydroxo-μ-phenoxodicopper(II) species, through the peroxo complex derived from the reaction with dioxygen. In the same system, xylyl ligand hydroxylation can also be achieved by treatment of the dinuclear $Cu^{II}$ complex $[Cu_2$(*m*-XYLpy$_2$)$]^{4+}$ with hydrogen peroxide.[30] The monooxygenase reaction by $Cu^{I}$ and dioxygen is not observed when the pyridine rings in the chelating arms of the *m*-xylyl-containing ligand are replaced by other nitrogen heterocycles such as imidazoles or benzimidazoles.[23,31−34] However, the dicopper(I) complex $[Cu_2$(L-66)$]^{2+}$, in which the ligand L-66 contains *N*-methylbenzimidazole rather than pyridine rings,[32] forms a peroxodicopper(II) complex capable of hydroxylating an exogenous phenol.[19] In addition, when $[Cu_2$(L-66)$]^{4+}$ is treated with hydrogen peroxide, the resulting hydroperoxodicopper(II) complexes effect double hydroxylation of the xylyl aromatic ring, to produce a hydroquinone complex.[34] In this paper we report structure and reactivity studies on the dicopper(I) and dicopper(II) complexes of the ligand L-55 (L-55 = α,α′-bis{bis[1-(1′-methyl-2′-benzimidazolyl)-

[a] Dipartimento di Chimica Generale, Università di Pavia, Via Taramelli 12, 27100 Pavia, Italy
Fax: (internat.) + 39-0382/528544
E-mail: bioinorg@unipv.it
[b] Dipartimento C.I.M.A., Università di Milano, Centro CNR, Via Venezian 21, 20133 Milano, Italy
[c] Dipartimento di Scienze Chimiche, Università di Trieste, Via L. Giorgieri 1, 34127 Trieste, Italy
[d] Institute of Inorganic Chemistry, University of Erlangen-Nürnberg, Egerlandstraße 1, 91058 Erlangen, Germany

methyl]amino}-*m*-xylene, Scheme 1),[35] which is related both to L-66, containing longer chains on the benzimidazolyl arms connected to the diamino-*m*-xylene unit, and to EBA, where a more flexible carbon chain replacing the *m*-xylyl unit[26] (Scheme 1). The synthesis and spectroscopic characterization of the copper(I) and copper(II) complexes of L-55 in solution have been reported before.[33,35] The X-ray crystal structure investigation of the $[Cu^{I}_2(L\text{-}55)(MeCN)_2](PF_6)_2$ (**1**) and $[Cu^{II}_2(L\text{-}55)(OMe)_2][ClO_4]_2$ (**2**) complexes reported here shows an extremely weak Cu−amine axial interaction, constrained by the small five-membered chelating ring units. This structural feature strongly affects the properties of the resulting copper complexes, particularly the reactivity patterns of the reduced and oxidized forms of the L-55 complexes towards dioxygen and hydrogen peroxide, respectively.

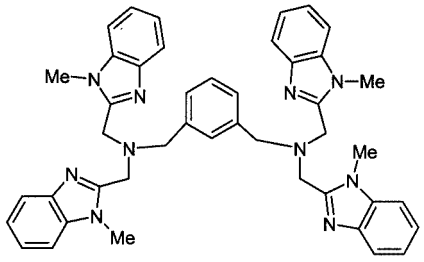

L - 55

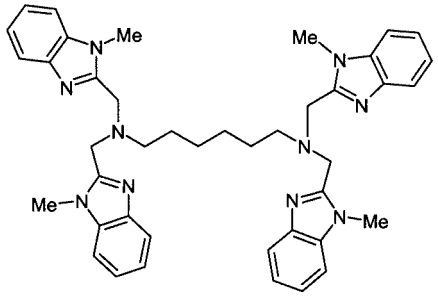

EBA

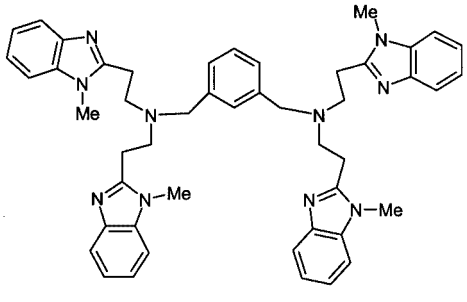

L- 66

Scheme 1

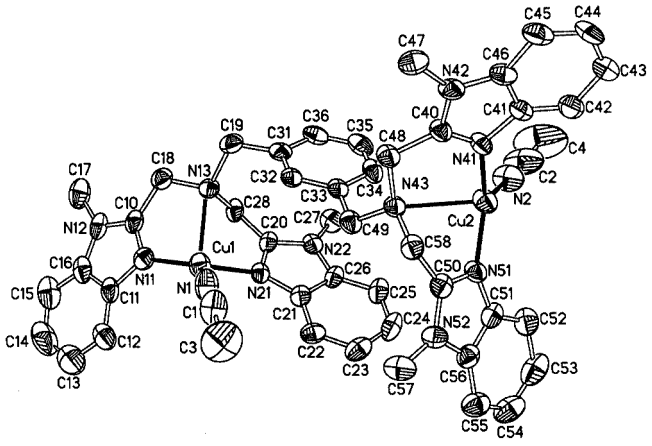

Figure 1. ORTEP[37] diagram of the cation **1** with the atom numbering labels

## Results and Discussion

### X-ray Structure of $[Cu^{I}_2(L\text{-}55)(MeCN)_2](PF_6)_2$ (1)

The structure of **1** consists of discrete $[Cu^{I}_2(L\text{-}55)(MeCN)_2]^{2+}$ cations and $PF_6^-$ anions. An ORTEP view of the cation, including the labelling scheme, is shown in Figure 1. The two crystallographically independent $Cu^{I}$ centers are three-coordinate with ligation from two benzimidazolyl N-donors and one acetonitrile N-donor, in a slightly distorted trigonal arrangement. The Cu−NCMe distances are slightly shorter than the other two. A long contact to the tertiary amino nitrogen donor [Cu1−N13, 2.602(5) Å, and Cu2−N43, 2.707(5) Å] is observed, the $N(sp^3)$ lone pair pointing approximately towards the copper ion; this may be indicative of a weak bonding interaction. The geometry around Cu is similar to the coordination around one copper(I) ion in a dinuclear complex derived from the ligand 1,3-bis[bis(2-pyridylmethy1)amino]benzene, although the Cu−N distance here is shorter [2.39(2) Å].[36] The geometry of **1** differs significantly from that found in the $[Cu^{I}_2(m\text{-}XYLpy_2)]^{2+}$ cation,[27] in which *m*-$XYLpy_2$ = $[(2\text{-}pyCH_2CH_2)_2N{-}CH_2C_6H_4CH_2{-}N(2\text{-}pyCH_2CH_2)_2]$. In the latter, in fact, each $Cu^{I}$ achieves tricoordination through ligation of two pyridyl donors at short distances, slightly more than 1.90 Å, and the $N(sp^3)$ amino donor at a long distance, around 2.2 Å. Furthermore, the planar arrangement of the N donors around the copper ions is dramatically distorted from ideal trigonal geometry towards a T-shaped geometry with an angle of about 150° between the two Cu−benzimidazolyl distances.

The differences observed in the $Cu^{I}$ coordination in the two cations may mainly be ascribed to the presence in $[Cu^{I}_2(L\text{-}55)(MeCN)_2]^{2+}$ of a methylene group bridging the $N(sp^3)$ atom to the benzimidazole residues. This does not allow ring-closure at a suitable Cu−$N(sp^3)$ coordination distance, as occurs in $[Cu^{I}_2(m\text{-}XYLpy_2)]^{2+}$, in which $N(sp^3)$ and the pyridyl moieties are joined by ethylene bridges. Consequently, the coordinatively unsaturated $Cu^{I}$ center binds an acetonitrile molecule, so the two $Cu^{I}$ ions in the two kinds of cations have dramatically different coor-

Table 1. Crystal data and structure refinement for $[Cu^{I}_2(L\text{-}55)(MeCN)_2](PF_6)_2\cdot 3MeCN$ [(**1**)·3MeCN] and $[Cu^{II}_2(L\text{-}55)(OMe)_2][ClO_4]_2\cdot 1.25MeOH$ (**2**)

| | | |
|---|---|---|
| Empirical formula | $C_{54}H_{59}Cu_2F_{12}N_{15}P_2$ | $C_{47.25}H_{50}Cl_2Cu_2N_{10}O_{11.25}$ |
| Formula mass | 1335.18 | 1135.95 |
| Temperature | 200(2) K | 293(2) K |
| Wavelength | 0.71073 Å | 0.71069 Å |
| Crystal system, space group | triclinic, $P\bar{1}$ | triclinic, $P\bar{1}$ |
| Unit cell dimensions | $a$ = 13.022(3) Å, α = 81.85(3)° | $a$ = 10.462(4) Å, α = 78.08(3)° |
| | $b$ = 13.944(3) Å, β = 74.18(3)° | $b$ = 13.226(4) Å, β = 89.18(3)° |
| | $c$ = 18.433(6) Å, γ = 69.02(1)° | $c$ = 20.149(7) Å, γ = 80.07(2)° |
| Volume | 3003(2) $Å^3$ | 2686.4(16) $Å^3$ |
| $Z$, calculated density | 2, 1.477 $Mg/m^3$ | 2, 1.404 $Mg/m^3$ |
| Absorption coefficient | 0.849 $mm^{-1}$ | 0.957 $mm^{-1}$ |
| $F$(000) | 1368 | 1171 |
| Crystal size | 0.50 × 0.40 × 0.30 mm | 0.6 × 0.4 × 0.4 mm |
| Reflections collected/unique | 12110/10581 [$R$(int) = 0.1246] | 9476/9449 [$R$(int) = 0.0230] |
| Refinement method | full-matrix, least-squares on $F^2$ | full-matrix, least-squares on $F^2$ |
| Data/restraints/parameters | 10578/17/797 | 9476/0/653 |
| Goodness-of-fit on $F^2$ | 0.936 | 1.057 |
| Final $R$ indices [$I > 2\sigma(I)$] | $R1$ = 0.0756, $wR2$ = 0.1850 | $R1$ = 0.0856, $wR2$ = 0.1958 |
| $R$ indices (all data) | $R1$ = 0.1414, $wR2$ = 0.2067 | $R1$ = 0.1950, $wR2$ = 0.2564 |
| Largest diff. peak and hole | 0.864 and −0.709 e·$Å^{-3}$ | 0.697 and −0.504 e·$Å^{-3}$ |

dinations and possibly different electronic configurations. Crystal data and structure refinement are given in Table 1. Complete tables of atomic parameters and bond lengths and angles are deposited with the CCDC.

### X-ray Structure of $[Cu^{II}_2(L\text{-}55)(OMe)_2][ClO_4]_2\cdot 1.25MeOH$ (2)

The crystals consist of dinuclear $[Cu^{II}_2(L\text{-}55)(OMe)_2]^{2+}$ cations and two $ClO_4^-$ anions. These crystals spontaneously formed from a methanolic solution of the bis(μ-hydroxo)-bridged complex $[Cu_2(L\text{-}55)(OH)_2][ClO_4]_2$. Crystal data and structure refinement are shown in Table 1, and an ORTEP drawing, together with the atom numbering scheme of the cation, is shown in Figure 2.[37] The cation has an approximate mirror symmetry, the mirror plane containing the two bridging OMe, C40, and C43 atoms. The structure of the cation is similar to that of $[Cu_2(EBA)(OH)_2]^{2+}$, in which the ligand has a flexible spacer of six methylene carbon atoms instead of the five carbon atoms of the L-55 ligand. Each Cu has a highly distorted square-pyramidal geometry and coordinates to the tertiary amine in the apical position and the two $sp^2$-N atoms of the tridentate arm in two *cis* basal positions. The other two equatorial positions are occupied by the bridging methoxy groups. (Figure 2). In spite of the different spacer, the overall geometries of the $N_5Cu_2O_2N_5$ moieties are very similar in L-55 and EBA derivatives, as are the coordination geometries about the metal ions. These are compared in Table 2, together with the length of the spacer (N5···N10) and the intermetallic distances.

The basal donors of Cu1 and Cu2 are coplanar within 0.013 and 0.005 Å, respectively, and the displacements of Cu1 and Cu2 out of their respective mean planes toward the apical N donor are 0.114(4) and 0.149(4) Å, respectively. The two $N_2O_2$ basal planes make a dihedral angle (β) of 19.1(2)°, very similar to that observed in the EBA derivative

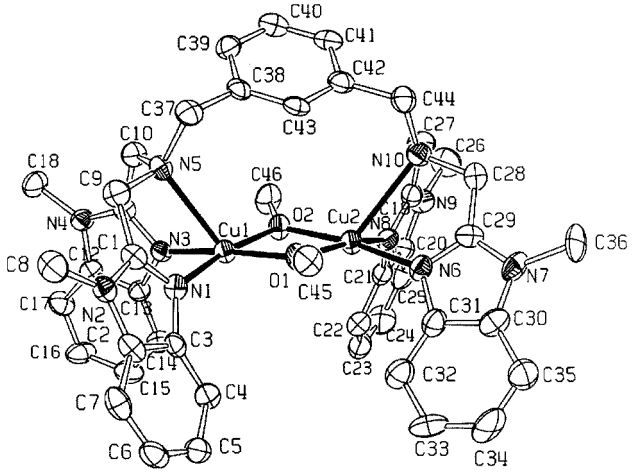


Figure 2. ORTEP[37] representation of the crystal structure of the cation **2**

[β = 20.0(2)°]. The geometry of the cation of **2** differs significantly from that reported for $[Cu_2L_3(OMe)_2]^{2+}$ [$L_3$ = (2-py$(CH_2CH_2)_2$N$(CH_2)_3$N(2-py$CH_2CH_2$py)$_2$],[38] which has a crystallographic mirror symmetry, the $L_3$ ligand having aminobis(2-$CH_2CH_2$-pyridyl) arms [instead of aminobis(2-$CH_2$-benzimidazolyl)ones] and a trimethylene spacer. The Cu coordination in the latter cation is less distorted than that in the cation of **2**, with a small shortening of the apical Cu−N distance of about 0.2 Å, and a small, but significant, lengthening of the basal distances of about 0.03 Å (Table 2). Correspondingly, the N($sp^3$)−N($sp^3$) distance is more than 1 Å shorter than that in the L-55 and EBA analogues. This is due to the large difference in the spacer length (Table 2) and to N($sp^3$)$(CH_2)_n$N($sp^3$) arms, as previously suggested.[26] Notwithstanding, the geometries of the $CuO_2Cu$ moieties are similar in the three dinuclear cations (Table 2). However, the *m*-xylyl plane in the cation of **2** is not parallel

Table 2. Comparison of coordination bond lengths and angles in $[Cu_2(L\text{-}55)(OMe)_2][ClO_4]_2$, $[Cu_2(EBA)(OH)_2][PF_6]_2$, and $[Cu_2L_3(OMe)_2][ClO_4]_2$

| | $[Cu_2(L\text{-}55)(OMe)_2][ClO_4]_2$ | $[Cu_2(EBA)(OH)_2][PF_6]_2$ | $[Cu_2L_3(OMe)_2][ClO_4]_2$ |
|---|---|---|---|
| Bond lengths [Å]: | | | |
| Cu1−O1 | 1.911(6) | 1.892(11) | 1.934(9) |
| Cu1−O2 | 1.913(6) | 1.941(10) | 1.934(8) |
| Cu1−N1 | 1.970(7) | 1.930(12) | 1.992(12) |
| Cu1−N3 | 1.957(7) | 1.918(13) | 2.004(14) |
| Cu1−N5 | 2.503(7) | 2.487(11) | 2.363(13) |
| Cu2−O1 | 1.926(6) | 1.882(10) | − |
| Cu2−O2 | 1.921(6) | 1.887(12) | − |
| Cu2−N6 | 1.947(7) | 1.942(11) | − |
| Cu2−N8 | 1.958(7) | 1.983(12) | − |
| Cu2−N10 | 2.586(8) | 2.548(11) | − |
| Cu1···Cu2 | 3.003(2) | 2.988(2) | 3.070(3) |
| N5···N10 | 6.096(10) | 6.050(15) | 4.75(1) |
| Bond angles [°]: | | | |
| O1−Cu1−O2 | 76.8(2) | 75.2(4) | 74.8(5) |
| O1−Cu1−N1 | 95.0(3) | 98.4(5) | 74.8(5) |
| O1−Cu1−N3 | 169.4(3) | 165.9(5) | 152.2(6) |
| O1−Cu1−N5 | 114.0(2) | 116.2(4) | 115.3(5) |
| O2−Cu1−N1 | 170.1(3) | 170.4(5) | 168.4(6) |
| O2−Cu1−N3 | 95.4(3) | 92.5(5) | 94.1(5) |
| O2−Cu1−N5 | 111.8(2) | 113.0(4) | 101.7(6) |
| N1−Cu1−N3 | 92.0(3) | 92.9(3) | 91.7(6) |
| N1−Cu1−N5 | 76.4(3) | 76.1(4) | 89.0(5) |
| N3−Cu1−N5 | 75.3(3) | 74.7(4) | 91.7(6) |
| Cu1−O1−Cu2 | 103.0(2) | 104.7(5) | 105.0(7) |
| Cu1−O2−Cu2 | 103.1(2) | 102.6(5) | 105.0(6) |
| O1−Cu2−O2 | 76.2(2) | 76.8(5) | − |
| O1−Cu2−N6 | 95.6(3) | 94.8(5) | − |
| O1−Cu2−N8 | 164.3(3) | 168.8(5) | − |
| O1−Cu2−N10 | 121.5(3) | 116.1(4) | − |
| O2−Cu2−N6 | 170.3(3) | 166.6(4) | − |
| O2−Cu2−N8 | 92.7(3) | 94.5(5) | − |
| O2−Cu2−N10 | 113.8(2) | 118.0(4) | − |
| N6−Cu2−N8 | 94.3(3) | 92.4(5) | − |
| N6−Cu2−N10 | 74.8(3) | 75.0(4) | − |
| N8−Cu2−N10 | 73.0(3) | 74.0(4) | − |

to the $CuO_2Cu$ mean plane {as it is to the propylene spacer carbon atom in $[Cu_2L_3(OMe)_2]^{2+}$}, making an interplanar angle of 31.7(3)°.

### Reactivity of L-55 Complexes: $Cu^I_2$ vs. $O_2$ and $Cu^{II}_2$ vs. $H_2O_2$

The reactivity of the $Cu^I$ complex $[Cu_2(L\text{-}55)(CH_3CN)_2]^{2+}$ toward dioxygen has been tested in different solvents and at various temperatures. When solutions of the complex are oxygenated at −85 °C in acetone, −90 °C in $CH_2Cl_2$, or −95 °C in THF, a moderately intense band near 350 nm (CT, $\varepsilon \approx 6000\ M^{-1}\cdot cm^{-1}$) and a weaker band at 500 nm (d-d envelope, $\varepsilon \approx 200\ M^{-1}\cdot cm^{-1}$) rapidly develop. In neither case can the reaction be reversed by application of vacuum/argon purge cycles, even upon mildly warming the solution. The UV band is bleached by the addition of a small excess of acid at low temperature, and no trace of hydrogen peroxide could be detected by peroxidase assay[19] after quenching of the reactions. Therefore, on reaction with dioxygen, $[Cu_2(L\text{-}55)(CH_3CN)_2]^{2+}$ does not produce a stable peroxo complex, but undergoes an irreversible oxidation to copper(II) species. Furthermore, application of the low-temperature stopped-flow method, a technique that has proved extremely useful for the spectroscopic detection of "copper−dioxygen adducts",[28,39] did not allow the observation of a peroxo intermediate complex. The spectral characteristics of the formed species are different from those of L-55 (hydroxo)dicopper(II) complexes that we have reported previously.[35] However, these oxygenated solutions are highly sensitive to moisture, and their UV/Vis spectra change quickly upon exposure to air, producing LMCT bands at 300 nm ($\varepsilon \approx 4300\ M^{-1}\cdot cm^{-1}$) and 335 nm ($\varepsilon \approx 3500\ M^{-1}\cdot cm^{-1}$), which testify to the formation of the previously characterized bis(hydroxo)dicopper(II) adduct.[35] The spectroscopic data and the sensitivity to water suggest that the low-temperature oxygenation of **1** affords a μ-oxodicopper(II) complex, which may be formed in a fast reaction as the $Cu_2O_2$ intermediate reacts with excess $Cu^I$ [Equation (1)].

$$Cu^I\cdots Cu^I + O_2 \rightarrow [Cu_2O_2] + Cu^I\cdots Cu^I \rightarrow 2\,Cu^{II}-O-Cu^{II} + H_2O \rightarrow 2\,Cu^{II}-(OH)_2-Cu^{II} \quad (1)$$

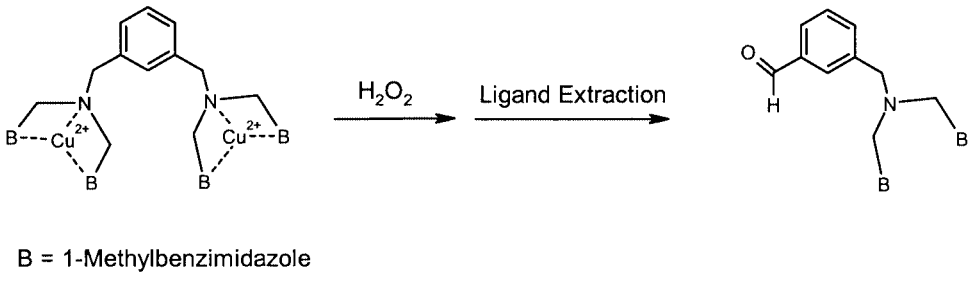


Scheme 2

The positions of the LMCT bands developing during the low-temperature experiments do, in fact, agree with those reported for other μ-oxodicopper(II) complexes.[40,41] The oxygenation behavior of $[Cu_2(EBA)]^{2+}$, in which the copper coordination set is identical to that of $[Cu_2(L\text{-}55)(CH_3CN)_2]^{2+}$, is also similar.[26] The extreme electrophilicity of the putative oxygen intermediate $[Cu_2O_2]$ is not unexpected in view of the structural features of **1** and **2**, in which essentially only two poorly basic benzimidazole nitrogen donors of the ligand are coordinated to the copper ions (Figures 1 and 2). With $[Cu_2(L\text{-}66)]^{2+}$, in contrast, a stable and reversible dioxygen complex is formed at low temperature.[19] In this case, the larger size and flexibility of the chelate rings allows the ligand to bind each $Cu^I$ with three nitrogen donors and the copper(I) centers to attain a more regular tetrahedral geometry. This is confirmed by the electrochemical data, which show that the ligand L-66 stabilizes the copper(I) state more than L-55 or EBA.[26,35] Furthermore, the ligand flexibility more easily supports the structural reorganization involved in the $Cu^{II}/Cu^I$ redox exchange.[35]

The reactivity of $[Cu_2(L\text{-}55)(H_2O)_2]^{4+}$ toward hydrogen peroxide was also investigated. A tenfold excess of $H_2O_2$, after 12 h reaction time at room temperature, produced a regiospecific hydroxylation of the ligand at one benzylic carbon atom, followed by decomposition of the complex, in 50% yield (Scheme 2). Isolation of the oxidized ligand showed the presence of an aldehyde group, with a characteristic $^1H$ NMR peak at $\delta \approx 10$ ppm. The loss of a chelating arm of the ligand was confirmed by ESI-MS analysis (see Exp. Sect.). It is interesting to note that in the related complex $[Cu_2(L\text{-}66)]^{4+}$,[34] and also in $[Cu_2(m\text{-}Xylpy_2)]^{4+}$,[30] hydrogen peroxide effects ligand hydroxylation at the central xylyl residue. Therefore, the coordination environment of $Cu^{II}$ centers, and in particular the five- or six-membered chelate ring size, plays a major role in effecting the hydroxylation reaction and in controlling the regiochemistry of C−H attack. Oxidative cleavage at the benzylic carbon atom, with production of an aromatic aldehyde, has previously been observed in the oxygenation of the $Cu^I$ complexes $[Cu(PhCH_2Py)_2]^+$ [41] and $[Cu_2(m\text{-}Xyl^{i\text{Pr}4})]^{2+}$.[42]

### Ligand Protonation and Stability Constants of Copper(II)−L-55 Complexes

The protonation and $Cu^{2+}$ complex-forming equilibria of the ligand L-55 were investigated potentiometrically in a mixture of acetonitrile/water (4:1, v/v). We were able to monitor five protonation steps for L-55 and to determine their cumulative logβ values as 8.04 (0.2), 14.94 (0.2), 19.85 (0.3), 23.98 (0.1), 25.85 (0.3). The ligand easily and simultaneously incorporates two copper(II) ions according to the equilibrium in Equation (2).

$$2\,Cu^{2+} + \text{L-55} \rightleftarrows [Cu_2(\text{L-55})]^{4+} \quad \log\beta_{120} = 20.62\,(0.1) \tag{2}$$

The stability constant of this complex is similar to that of the corresponding dinuclear $Cu^{II}$ complex derived from L-66 ($\log\beta_{120} = 19.89$[34]), while that of the $[Cu_2(EBA)]^{4+}$ complex is much larger ($\log\beta_{120} = 37.68$[26]), indicating that the longer and flexible carbon chain of EBA enables the repulsion between the positively charged cationic centers to be reduced.

With increasing pH, the two copper ions, each containing coordinated water molecules, undergo stepwise deprotonation of coordinated water molecules, as shown in the species distribution diagram in Figure 3, according to the equilibria in Equation (3) and (4) which occur with $pK_a$ values of 6.93 and 6.25, respectively.

$$[Cu_2(\text{L-55})(H_2O)_2]^{4+} \rightleftarrows [Cu_2(\text{L-55})(H_2O)(OH)]^{3+} + H^+ \tag{3}$$

$$[Cu_2(\text{L-55})(H_2O)(OH)]^{3+} \rightleftarrows [Cu_2(\text{L-55})(OH)_2]^{2+} + H^+ \tag{4}$$

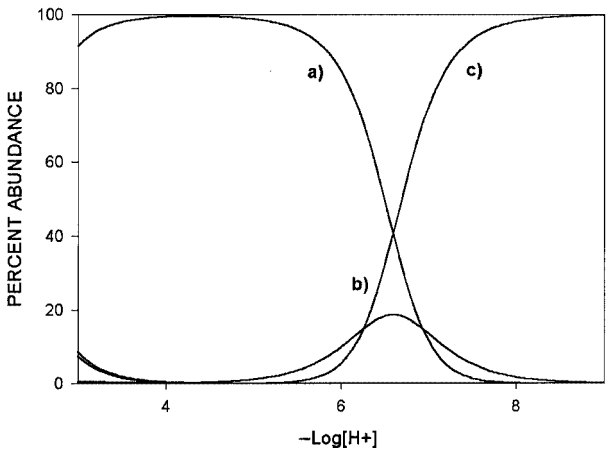


Figure 3. Species distribution in the 2Cu/L-55 system as a function of pH in acetonitrile/water solution: a) $[Cu_2(L\text{-}55)(H_2O)_2]^{4+}$; b) $[Cu_2(L\text{-}55)(H_2O)(OH)]^{3+}$; c) $[Cu_2(L\text{-}55)(OH)_2]^{2+}$

Both p$K_a$ values are rather low and consistent with the formation of a bis(μ-hydroxo)dicopper(II) species. It may be noted that the second deprotonation occurs with lower p$K_a$ values, even though the charge decreases after the first step. This behavior is not surprising. As is suggested by the X-ray crystal structure of $[Cu_2(L\text{-}55)(OMe)_2][ClO_4]_2$ (**2**), formation of the bis(μ-hydroxo) bridge probably drives proton dissociation, accounting for p$K_{a2}$ < p$K_{a1}$. Therefore, as we have previously noted,[26] the monohydroxo species that forms after the first deprotonation step preorganizes the complex and facilitates the formation of the dibridged complex containing the ring-closed $Cu_2(OH)_2$ core. Deprotonation of coordinated water in the related complex $[Cu_2(EBA)(OH)_2]^{4+}$ follows the same trend (p$K_{a2}$ < p$K$a1), but both p$K_a$ values are larger.[26] This indicates that the *m*-xylyl residue of L-55 more readily favors the adoption of the folded conformation, stabilizing the bis(μ-hydroxo) bridge with respect to the long aliphatic chain of EBA.

### NMR Studies on Copper(II)−L55 Complexes

The pH-driven equilibrium between $[Cu_2(L\text{-}55)(H_2O)_2]^{4+}$ (**3**) and its bis(μ-hydroxo) adduct **4** reported above can conveniently be monitored by $^1$H NMR spectroscopy. The $^1$H NMR spectrum of **3** in DMSO solution shows typical paramagnetic behavior, with broad signals (Figure 4a) resulting from the presence of only weakly coupled metal centers. The unresolved and broad peaks are spread between δ = 30 and −3 ppm, and increasing temperature shifts the downfield resonances towards the diamagnetic region, obeying Curie behavior, as shown in Figure 5a. In agreement with the above interpretation, the $\mu_{eff}$/Cu was 1.27 $\mu_B$, confirming the existence of a moderate interaction between the copper centers. This interaction is probably mediated by bridging water molecule(s) between the dicopper(II) centers. The addition of 2 equiv. of $OH^-$ to the DMSO solution of **3** completely changes the NMR spectral shape. Formation of the bis(μ-hydroxo) bridge in **4** strongly increases the ex-

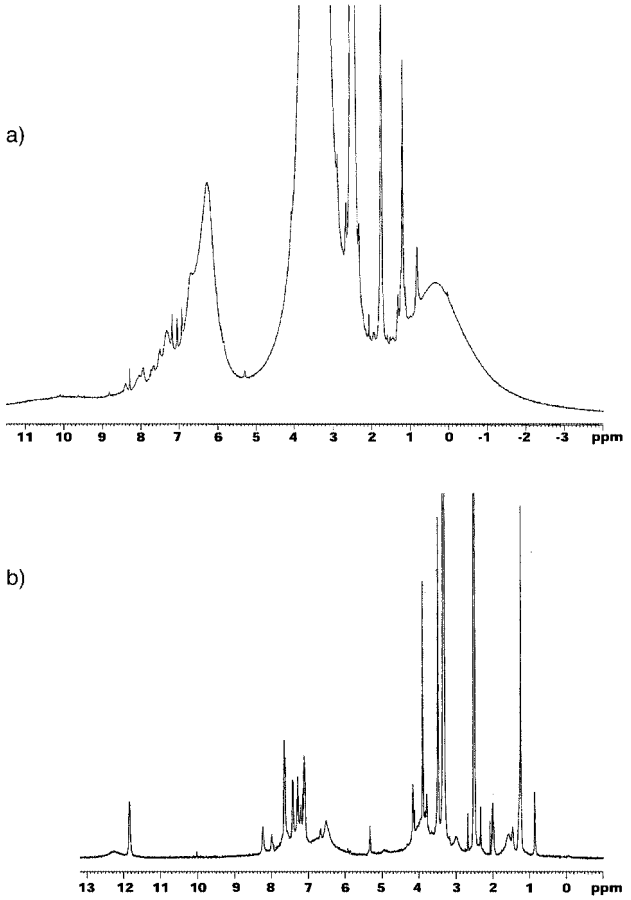


Figure 4. Diamagnetic regions of the $^1$H NMR (δ values, ppm) spectra of $[Cu_2(L\text{-}55)(H_2O)_2]^{4+}$ and $[Cu_2(L\text{-}55)(OH)_2]^{2+}$ in DMSO solutions (1.5 mM) at 25 °C

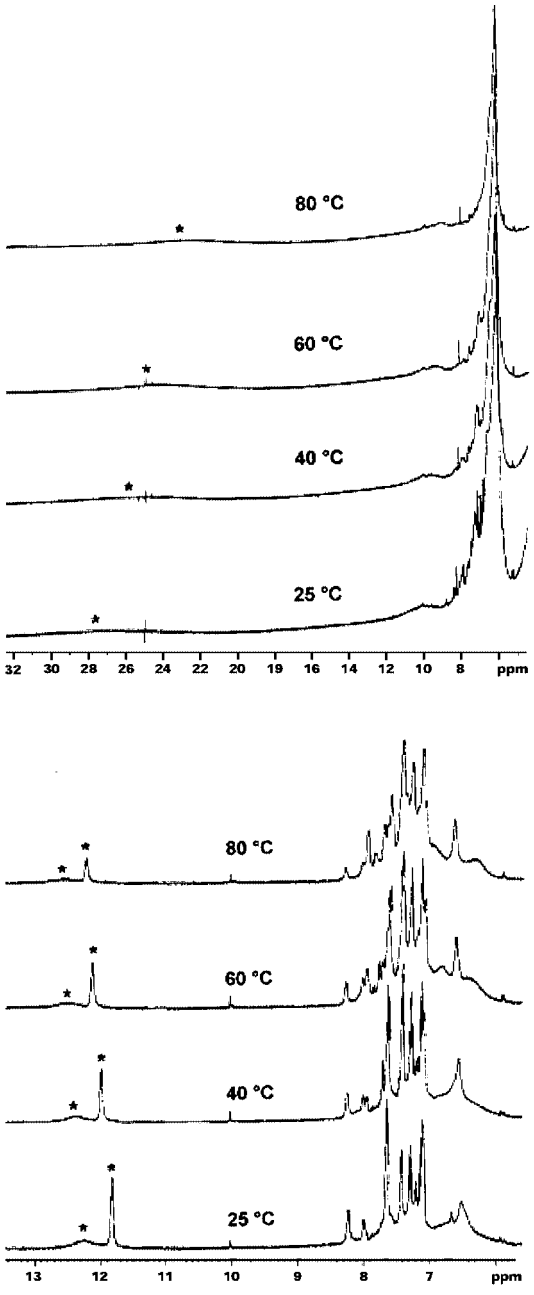


Figure 5. Upfield shifted resonances of a) $[Cu_2(L\text{-}55)(H_2O)_2]^{4+}$ and b) $[Cu_2(L\text{-}55)(OH)_2]^{2+}$; $^1$H NMR spectra were recorded in DMSO at different temperatures

change interaction between the metal centers. The compound gives a diamagnetic-type NMR spectrum in which broadening of the peaks is reduced dramatically (Figure 4b), and the signals are detected only between $\delta = 0$ and 14 ppm. The temperature dependence of these signals was studied over the temperature range between 25 and 80 °C. As shown in Figure 5b, the downfield resonances clearly shift away from the diamagnetic region as the temperature increases, obeying anti-Curie law behavior. The magnetic properties of **4** in solution were confirmed by the Evans susceptibility method. At 25 °C, $\mu_{eff}$/Cu was reduced to 0.47 $\mu_B$, indicating a strong exchange coupling between the copper(II) centers. In the bridged bis(μ-hydroxo)dicopper(II) complexes the exchange interaction between the electron spins of the metal ions affects both the relaxation and the paramagnetic shift properties.[43,44] Hence, $^1$H NMR spectroscopy strongly confirms the double-bridged structure of $[Cu_2(L\text{-}55)(OH)_2]^{2+}$ in solution, which should be clearly similar to those reported for **2** and $[Cu_2(EBA)(OH)_2]^{2+}$.[26] It can be noted that this coordination arrangement for $[Cu_2(L\text{-}55)(OH)_2]^{2+}$ was previously postulated on the basis of UV/Vis titration data.[35]

## Conclusion

The reaction between $[Cu^I_2(L\text{-}55)(MeCN)_2]^{2+}$ and dioxygen produces $[Cu^{II}_2(L\text{-}55)(OH)_2]^{2+}$ through the formation of a species that we formulate as the μ-oxo-bridged complex $[Cu^{II}_2(L\text{-}55)O]^{2+}$, on the basis of its spectral properties and reaction with water. With $[Cu^I_2(L\text{-}66)]^{2+}$, in contrast, the isolation and characterization of the $[Cu_2(L\text{-}66)O_2]^{2+}$ peroxo complex at low temperatures was possible.[19] On raising the temperature, this peroxo complex also undergoes a similar irreversible oxidation (Scheme 3, a). However, when $[Cu^I_2(m\text{-}Xylpy_2)]^{2+}$ reacts with $O_2$, the resulting $Cu_2O_2$ complex effects a hydroxylation of the aromatic ring (Scheme 3b), giving a five-coordinate μ-phenoxo,μ-hydroxo-bridged dicopper(II) complex.[27] Structural results for compounds **1** and **2**, in comparison with those for the corresponding *m*-Xylpy$_2$ complexes, suggest that the different behavior of the Cu$^I$ species toward dioxygen should be principally related to the different structural environments of the Cu$^I$ ions, in spite of the apparently favorable orientation of the xylyl ring. Although the structure of the starting Cu$^I$ compound is not known, the Cu$^I$−EBA complex should behave like the L-55 derivative, as suggested by the long Cu···N(amine) distance found in Cu$^{II}$−EBA,[26] close to that found for **2**. The reactivity of the putative dioxygen intermediates involved in the reaction pathways of L-55 and EBA complexes (Scheme 3a) are strictly related to their structural features. The absent or weak axial interaction offered by the amine group of the ligands increases the electrophilic reactivity of the $[Cu_2O_2]^{2+}$ moiety. Even at low temperature, as soon as the $[Cu_2(L\text{-}55)O_2]^{2+}$ or $[Cu_2(EBA)O_2]^{2+}$ complexes form, they probably react rapidly with excess Cu$^I$ species present in solution (Scheme 3a), producing their corresponding μ-oxodicopper(II) complexes.

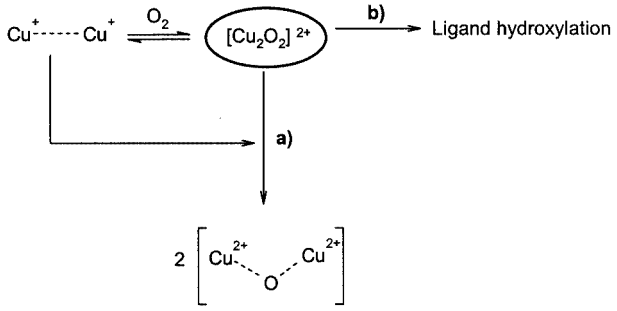


Scheme 3

The reactivity of the Cu$^{II}$ complexes with hydrogen peroxide also elicits important differences in the behavior of L-55 vs. L-66 or *m*-Xylpy$_2$ complexes. In the last two cases, in fact, formation of a hydroperoxo intermediate results in hydroxylation of the central *m*-xylyl ring.[30,34] With $[Cu_2(L\text{-}55)(H_2O)_2]^{4+}$ a similar reaction through a putative μ-hydroperoxodicopper(II) complex seems possible, judging from the crystal structure of **2**, but the observed hydroxylation is much slower and occurs at the benzylic position. To clarify these differences, our current efforts are directed to the characterization of the so far elusive hydroperoxo intermediate formed by $[Cu_2(L\text{-}55)(H_2O)_2]^{4+}$.

## Experimental Section

**General:** All reagents were purchased from commercial sources and were used as received unless otherwise noted. The ligand L-55 and the corresponding dinuclear copper(I) and copper(II) complexes studied here were prepared by published procedures.[33,35] NMR spectra were recorded with a Bruker Avance 400 spectrometer. Optical spectra were measured with HP 8452A and 8453 diode array spectrophotometers. Electrospray ionization MS spectra were acquired with a Finnigan MAT system equipped with an ion trap detector. Solutions were introduced into the electrospray source by syringe pump at 10 μL·min$^{-1}$. The ESI source was operated at 3.5 kV, the capillary temperature was set at 180 °C, and its voltage at 10 V; the experiments were performed in positive ion mode.

**Single-Crystal X-ray Structure Determination of 1:** Crystals of **1** were obtained by diffusion of diethyl ether into a solution of **1** in acetonitrile under an inert gas. Single crystals were coated with polyfluoropolyalkyl ether oil and mounted on a glass fiber. Data were collected with a Siemens P4 diffractometer. Lorentz and polarization corrections were applied. The structures were solved by direct methods and refined on $F^2$ by full-matrix, least-squares techniques.[45] Non-hydrogen atoms were refined with anisotropic thermal parameters. The $PF_6^-$ anions are partly situated on inversion centers and disordered; they were refined by use of SIMU restraints. All hydrogen atoms are positioned geometrically. No hydrogen atoms were included in the description of three not very well defined acetonitrile solvate molecules.

**Single-Crystal X-ray Structure Determination of 2:** The crystals used in the X-ray analysis were grown by slow concentration of a methanol solution of $[Cu_2(L\text{-}55)(OH)_2][ClO_4]_2$. For data collection, a crystal of 0.6 × 0.4 × 0.4 mm, sealed in a glass capillary tube, in the presence of mother liquor, was used. The diffraction data were

collected at room temperature with an Enraf−Nonius CAD4 four-circle automated diffractometer with graphite-monochromated Mo-$K_\alpha$ radiation. Accurate unit cell parameters and orientation matrix were determined by least-squares refinement of the setting angles of 25 well-centered reflections in the range $22° < 2\theta < 30°$. Reflections were collected in the ω/2θ-scan mode. No decay was observed throughout the data collection. Correction for Lorentz polarization and scan absorption was applied. A total of 9476 (9449 independent) reflections were collected, 4424 of which having $I > 2\sigma(I)$. Unit cell parameters are $a$ = 10.462(4), $b$ = 13.226(4), $c$ = 20.149(7) Å, α= 78.08(3), β= 89.18(3), and γ = 80.07(2)° for the triclinic $P\bar{1}$ space group, $V$ = 2686.4(16) Å$^3$, $Z$ = 2, $M_w$ = 1135.9 and $D_{calcd.}$ = 1.404 Mg/m$^3$. The structure was solved by conventional Patterson and Fourier methods and refined by least-squares methods.[46,47] All the non-H atoms were treated anisotropically, except those of the solvent methanol, and the H atom contribution was held constant in the final refinement of 653 parameters. The final $R$ index was 0.086 ($Rw$ = 0.196) for reflections with $I > 2\sigma(I)$. Crystal collection and refinement data are given in Table 1. Complete tables of atomic parameters and bond lengths and angles are deposited with the CCDC. CCDC-198231 (**2**) and -198232 (**1**) contain the supplementary crystallographic data for this paper. These data can be obtained free of charge at www.ccdc.cam.ac.uk/conts/retrieving.html [or from the Cambridge Crystallographic Data Centre, 12 Union Road, Cambridge CB2 1EZ, UK; Fax: (internat.) + 44-1223/336-033; E-mail: deposit@ccdc.cam.ac.uk].

**Low-Temperature Spectroscopy:** Low-temperature spectra (−80 °C and below) recorded during the reaction between $[Cu_2(L\text{-}55)(CH_3CN)_2]^{2+}$ and dioxygen were obtained with a custom-designed immersible fiber-optic quartz probe (Hellma) fitted to a Schlenk vessel and connected with an HP 8452A diode array spectrophotometer. Experiments were performed by bubbling chilled dioxygen into ca. 1.5 mM solutions of the complexes, formed in situ by mixing stoichiometric amounts of ligand and copper(I) BArF salt {BArF = $[\{3,5\text{-}(CF_3)_2C_6H_3\}_4B]^-$} in the appropriate solvent.[40,48]

**Potentiometric Determinations:** Potentiometric determination of L-55 in the absence and in the presence of copper(II) ions were performed with an apparatus and by methods described elsewhere[49] in 50 mL of an acetonitrile/water mixture (80:20, v/v) made up to 0.1 M in ionic strength with $NaClO_4$ at 298 K. The electrodes were dipped in the above solvent mixture for more than 1 h before standardization of the system, which was also made as described previously.[49] The HYPER-QUAD program was used to process the data to calculate both the protonation and stability constant.[50]

**Solution Susceptibility Measurements:** The susceptibility of the sample was measured by the modified Evans method.[51,52] A coaxial NMR tube was used with *tert*-butyl alcohol as an internal reference. The solution of the paramagnetic species (5 mM, DMSO) of which the susceptibility was to be determined was introduced into the inner narrow-bore tube, while the solvent containing the reference compound (4%, v/v) was placed into the outer tube. The paramagnetic solution also contained the reference compound, in an identical amount. The methyl proton signals of *tert*-butyl alcohol were recorded and the separation of the two signals ($\Delta\nu$) was monitored and regarded as the paramagnetic shift. Mass susceptibility ($\chi_p$) is correlated to the above measured $\Delta\nu$ as given in Equation (5) where $c$ is the concentration of the solution (mol/L), $M$ the molecular weight of the complex, $\nu_0$ the operating rf of the spectrometer, and $\chi_0$ the susceptibility of pure solvent.

$$\chi_p = \chi_0 + \frac{3000 \cdot \Delta\nu}{4\pi\nu_0 cM} \quad (5)$$

Molar susceptibility ($\chi_M$) can then be calculated after the usual correction.[53] The magnetic moment in solution ($\mu_{eff}$) was obtained from the same shift data as reported in the literature.[54] The reliability of our measurement method was tested with $CuSO_4 \cdot 5H_2O$ as paramagnetic standard. The $\chi_p$, $\chi_M$, $\mu_{eff}$ values for this compound agreed perfectly with those previously calculated and available in the literature.[51,52]

**Isolation of the Hydroxylated Ligand:** The complex $[Cu_2(L\text{-}55)(H_2O)_2]^{4+}$ (100 mg, 0.07 mmol) was dissolved in a mixture of MeOH/phosphate buffer (50 mM, pH = 7, 8:2, v/v), and a concd. aqueous solution of hydrogen peroxide (0.7 mmol) was added. The solution was allowed to react for 12 h whilst stirring at room temperature. It was then concentrated under reduced pressure and chromatographed on a Sephadex LH-20 column (1.5 × 40 cm). The resulting fraction was collected, and the solvent volume was reduced by rotary evaporation and added to 100 mL of a mixture of concentrated ammonia/$CH_2Cl_2$ (1:1, v/v). The aqueous layer was separated and further extracted with cold $CH_2Cl_2$ (50 mL, 3 times). The organic extracts were combined, washed with water, and dried with $MgSO_4$. The final organic mixture was purified by silica gel column, by eluting with a mixture of $CH_2Cl_2$/MeOH (9:1, v/v) to which an increasing amount of concentrated $NEt_3$, from 1 to 15%, was added. The fraction containing the product was collected by spectrophotometric monitoring of the UV absorptions of the benzimidazole ring (284, 276, 254 nm) in the eluate, and after evaporation of the solvent afforded a light yellow, unstable oil (overall yield 50%). $^1$H NMR ($CDCl_3$): δ = 9.8 (s, 1 H, HCO), δ = 7.6 (m, 8 H, Bz + Xy), 4.1 (t, 4 H, $CH_2$), 3.9 (s, 2 H, $CH_2$-Xy), 3.6 (s, 6 H, $CH_3$-Bz) ppm. ESI-MS: $m/z$ = 424.4 $[L + H]^+$.

## Acknowledgments

The authors thank the Italian CNR, the University of Pavia (FAR), and COST for support. S. S. gratefully acknowledges financial support from the DFG and Prof. Rudi van Eldik (University of Erlangen-Nürnberg).

[1] A. G. Blackman, W. B. Tolman, *Struct. Bonding* **2000**, *97*, 179−211.
[2] K. D. Karlin, A. D. Zuberbühler, in: *Bioinorganic Catalysis*, 2nd ed., revised and expanded (Eds.: J. Reedijk, E. Bouwman), Dekker, New Jork, **1999**, pp. 469−534.
[3] S. Schindler, *Eur. J. Inorg. Chem.* **2000**, 2311−2326.
[4] H.-C. Liang, M. Dahan, K. D. Karlin, *Curr. Opin. Chem. Biol.* **1999**, *3*, 168−175.
[5] E. I. Solomon, P. Chen, M. Metz, S.-K. Lee, A. E. Palmer, *Angew. Chem. Int. Ed.* **2001**, *40*, 4570−4590.
[6] E. I. Solomon, U. M. Sundaram, T. E. Machonkin, *Chem. Rev.* **1996**, *96*, 2563−2605.
[7] M. A. McGuirl, D. M. Dooley, *Curr. Opin. Chem. Biol.* **1999**, *3*, 138−144.
[8] H. Decker, R. Dillinger, F. Tuczek, *Angew. Chem. Int. Ed.* **2000**, *39*, 1591−1595.
[9] P. L. Holland, W. B. Tolman, *Coord. Chem. Rev.* **1999**, *190−192*, 855−869.
[10] P. Gamez, P. G. Aubel, W. L. Driessen, J. Reedijk, *Chem. Soc. Rev.* **2001**, *30*, 376−385.
[11] C. S. Foote, J. S. Valentine, A. Greenberg, J. F. Liebman, *Active Oxygen in Chemistry*, Chapman & Hall, London, **1995**.
[12] K. D. Karlin, M. S. Nasir, B. I. Cohen, R. W. Cruse, S. Kaderli,

A. D. Zuberbühler, *J. Am. Chem. Soc.* **1994**, *116*, 1324−1336.
[13] E. Pidcock, H. V. Obias, C. X. Zhang, K. D. Karlin, E. I. Solomon, *J. Am. Chem. Soc.* **1998**, *120*, 7841−7847.
[14] P. L. Holland, K. R. Rodgers, W. B. Tolman, *Angew. Chem. Int. Ed.* **1999**, *38*, 1139−1142.
[15] J. A. Halfen, V. G. Young, Jr., W. B. Tolman, *Inorg. Chem.* **1998**, *37*, 2102−2103.
[16] S. Itoh, M. Taki, H. Nakao, P. L. Holland, W. B. Tolman, L. Que, Jr., S. Fukuzumi, *Angew. Chem. Int. Ed.* **2000**, *39*, 398−400.
[17] V. Mahadevan, J. L. DuBois, B. Hedman, K. O. Hodgson, T. D. P. Stack, *J. Am. Chem. Soc.* **1999**, *121*, 5583−5584.
[18] V. Mahadevan, M. J. Henson, E. I. Solomon, T. D. P. Stack, *J. Am. Chem. Soc.* **2000**, *122*, 10249−10250.
[19] L. Santagostini, M. Gullotti, E. Monzani, L. Casella, R. Dillinger, F. Tuczek, *Chem. Eur. J.* **2000**, *6*, 519−522.
[20] S. Itoh, H. Kumei, M. Taki, S. Nagatomo, T. Kitagawa, S. Fukuzumi, *J. Am. Chem. Soc.* **2001**, *123*, 6708−6709.
[21] L. Casella, M. Gullotti, G. Pallanza, R. Rigoni, *J. Am. Chem. Soc.* **1988**, *110*, 4221−4227.
[22] O. J. Gelling, F. van Bolhuis, A. Meetsma, B. L. Feringa, *J. Chem. Soc., Chem. Commun.* **1988**, 552−554.
[23] T. N. Sorrell, V. A. Vankai, M. L. Garrity, *Inorg. Chem.* **1991**, *30*, 207−210.
[24] G. Alzuet, L. Casella, M. Villa, O. Carugo, M. Gullotti, *J. Chem. Soc., Dalton Trans.* **1997**, 4789−4794.
[25] D. Ghosh, P. Mukherjee, *Inorg. Chem.* **1998**, *37*, 6597−6605.
[26] E. Monzani, G. Battaini, A. Perotti, L. Casella, M. Gullotti, L. Santagostini, G. Nardin, L. Randaccio, S. Geremia, P. Zanello, G. Opromolla, *Inorg. Chem.* **1999**, *38*, 5359−5369.
[27] K. D. Karlin, J. C. Hayes, Y. Gultneh, R. W. Cruse, T. W. McKown, J. P. Hutchinson, J. Zubieta, *J. Am. Chem. Soc.* **1984**, *106*, 2121−2128.
[28] K. D. Karlin, S. Kaderli, A. D. Zuberbühler, *Acc. Chem. Res.* **1997**, *30*, 139−147.
[29] M. Becker, S. Schindler, K. D. Karlin, T. A. Kaden, S. Kaderli, T. Palanche, A. D. Zuberbühler, *Inorg. Chem.* **1999**, *38*, 1989−1995.
[30] R. W. Cruse, S. Kaderli, C. J. Meyer, A. D. Zuberbühler, K. D. Karlin, *J. Am. Chem. Soc.* **1988**, *110*, 5020−5024.
[31] T. N. Sorrell, M. L. Garrity, *Inorg. Chem.* **1991**, *30*, 210−215.
[32] L. Casella, M. Gullotti, R. Radaelli, P. Di Gennaro, *J. Chem. Soc., Chem. Commun.* **1991**, 1611−1612.
[33] L. Casella, E. Monzani, M. Gullotti, D. Cavagnino, G. Cerina, L. Santagostini, R. Ugo, *Inorg. Chem.* **1996**, *35*, 7516−7525.
[34] G. Battaini, E. Monzani, A. Perotti, C. Para, L. Casella, L. Santagostini, M. Gullotti, R. Dillinger, C. Näther, F. Tuczek, *J. Am. Chem. Soc.*, submitted for publication.
[35] L. Casella, O. Carugo, M. Gullotti, S. Garofani, P. Zanello, *Inorg. Chem.* **1993**, *32*, 2056−2057.
[36] S. Schindler, D. J. Szalda, C. Creutz, *Inorg. Chem.* **1992**, *31*, 2255−2264.
[37] C. K. Johnson, *Report ORNL-5138, ORTEP*, Oak Ridge National Laboratory, Oak Ridge, TN, **1976**.
[38] K. D. Karlin, J. Shi, J. C. Hayes, J. W. McKown, J. P. Hutchinson, J. Zubieta, *Inorg. Chim. Acta* **1984**, *91*, L3−L7.
[39] M. Weitzer, M. Schatz, F. Hampel, F. W. Heinemann, S. Schindler, *J. Chem. Soc., Dalton Trans.* **2002**, 686−694.
[40] H. V. Obias, Y. Lin, N. N. Murthy, E. Pidcock, E. I. Solomon, M. Ralle, N. J. Blackburn, Y.-M. Neuhold, A. D. Zuberbühler, K. D. Karlin, *J. Am. Chem. Soc.* **1998**, *120*, 12960−12961.
[41] I. Sanyal, M. Mahroof-Tahir, M. S. Nasir, P. Ghosh, B. I. Cohen, Y. Gultneh, R. W. Cruse, A. Farooq, K. D. Karlin, S. Liu, J. Zubieta, *Inorg. Chem.* **1992**, *31*, 4322−4332.
[42] S. Mahapatra, S. Kaderli, A. Llobet, Y.-M. Neuhold, T. Palanche, J. A. Halfen, V. G. Young, Jr., T. A. Kaden, L. Que, A. D. Zuberbühler, W. B. Tolman, *Inorg. Chem.* **1997**, *36*, 6343−6356.
[43] V. Clementi, C. Luchinat, *Acc. Chem. Res.* **1998**, *31*, 351−361.
[44] N. N. Murthy, K. D. Karlin, I. Bertini, C. Luchinat, *J. Am. Chem. Soc.* **1997**, *119*, 2156−2162.
[45] G. M. Sheldrick, Siemens Analytical X-ray Inst., Inc., WI, USA, **1994**.
[46] G. M. Sheldrick, Universität Göttingen, Göttingen, Germany, **1993**.
[47] G. M. Sheldrick, *Acta Crystallogr., Sect. A* **1990**, *A46*, 467−473.
[48] M. Brookhart, B. Brant, A. F. Volpe Jr., *Organometallics* **1992**, *11*, 3920−3922.
[49] E. Monzani, L. Quinti, A. Perotti, L. Casella, M. Gullotti, L. Randaccio, S. Geremia, G. Nardin, P. Faleschini, G. Tabbi, *Inorg. Chem.* **1998**, *37*, 553−562.
[50] A. Sabatini, A. Vacca, P. Gans, *Coord. Chem. Rev.* **1992**, *120*, 389−405.
[51] D. F. Evans, *J. Chem. Soc.* **1959**, 2003−2005.
[52] S. K. Sur, *J. Magn. Reson.* **1989**, *82*, 169−173.
[53] R. L. Carlin, *Magnetochemistry*, Springer, New York, **1986**.
[54] I. Bertini, C. Luchinat, *NMR of Paramagnetic Substances*, Elsevier, Amsterdam, **1996**.

Received September 2, 2002
[I02493]